Am J Physiol Cell Physiol 288: C747–C756, 2005.
First published October 20, 2004; doi:10.1152/ajpcell.00420.2004.

Dynamic fibroblast cytoskeletal response to subcutaneous tissue stretch ex vivo and in vivo

Helene M. Langevin,[1] Nicole A. Bouffard,[1] Gary J. Badger,[2] James C. Iatridis,[3] and Alan K. Howe[4]

[1]*Department of Neurology,* [2]*Department of Medical Biostatistics,* [3]*Department of Mechanical Engineering, and* [4]*Department of Pharmacology, Vermont Cancer Center, University of Vermont College of Medicine, Burlington, Vermont*

Submitted 25 August 2004; accepted in final form 19 October 2004

Langevin, Helene M., Nicole A. Bouffard, Gary J. Badger, James C. Iatridis, and Alan K. Howe. Dynamic fibroblast cytoskeletal response to subcutaneous tissue stretch ex vivo and in vivo. *Am J Physiol Cell Physiol* 288: C747–C756, 2005. First published October 20, 2004; doi:10.1152/ajpcell.00420.2004.—Cytoskeleton-dependent changes in cell shape are well-established factors regulating a wide range of cellular functions including signal transduction, gene expression, and matrix adhesion. Although the importance of mechanical forces on cell shape and function is well established in cultured cells, very little is known about these effects in whole tissues or in vivo. In this study we used ex vivo and in vivo models to investigate the effect of tissue stretch on mouse subcutaneous tissue fibroblast morphology. Tissue stretch ex vivo (average 25% tissue elongation from 10 min to 2 h) caused a significant time-dependent increase in fibroblast cell body perimeter and cross-sectional area (ANOVA, $P < 0.01$). At 2 h, mean fibroblast cell body cross-sectional area was 201% greater in stretched than in unstretched tissue. Fibroblasts in stretched tissue had larger, "sheetlike" cell bodies with shorter processes. In contrast, fibroblasts in unstretched tissue had a "dendritic" morphology with smaller, more globular cell bodies and longer processes. Tissue stretch in vivo for 30 min had effects that paralleled those ex vivo. Stretch-induced cell body expansion ex vivo was inhibited by colchicine and cytochalasin D. The dynamic, cytoskeleton-dependent responses of fibroblasts to changes in tissue length demonstrated in this study have important implications for our understanding of normal movement and posture, as well as therapies using mechanical stimulation of connective tissue including physical therapy, massage, and acupuncture.

mechanotransduction; connective tissue; tensegrity; musculoskeletal manipulations; acupuncture

CYTOSKELETON-DEPENDENT CHANGES in cell shape are known to have profound effects on many cellular functions. A vast and growing literature has shown the importance of cytoskeletal regulation on nearly every fundamental biochemical process and cellular event (4, 24–26). It is also becoming increasingly apparent that both mechanical forces generated within the cytoskeleton of cells and externally applied forces are important determinants of both cell shape and cell function (10). Mechanotransduction—the ability of cells to perceive and biochemically interpret these forces—is an area of intense study and growing importance, given its pivotal role in signal transduction and cell function. Indeed, the effect of mechanical forces on cell shape is emerging as a key regulatory mechanism at the cellular, tissue, and organ levels.

Although the importance of internal and external mechanical forces on cell function and shape is well recognized, the near totality of evidence supporting these concepts is from cell culture experiments. Fibroblasts grown in cell culture have a markedly different appearance depending on whether they are grown on a two-dimensional (2D) vs. a three-dimensional (3D) matrix and whether this matrix is restrained (mechanically loaded) or floating (20). Cultured fibroblasts take on a "dendritic" phenotype (small globular cell bodies and long branching processes) when grown on 3D matrices but develop expanded, flatter cell bodies with shorter processes when grown on planar surfaces (19). Importantly, switching between these different phenotypes is associated with differential activation of signaling pathways such as activation of Rho kinase (37). Although the dendritic phenotype is thought to correspond to the natural "resting state" of fibroblasts, whereas the "sheetlike" phenotype is thought to be induced by mechanical stimulation or injury (20), this has not been verified in whole tissue ex vivo or in vivo.

The primary objective of this study was to characterize the response of fibroblasts to stretching of loose connective tissue. Loose connective tissue forms a continuous network throughout the body, including subcutaneous and interstitial connective tissues surrounding and permeating muscles and organs. Therapeutic mechanical deformation of loose connective tissue is used routinely in physiotherapy (e.g., in stress-relaxation techniques), as well as in many "alternative" therapies such as massage, myofascial release, and osteopathic and chiropractic manipulations. In addition, acupuncture was recently shown to cause winding, pulling, and deformation of subcutaneous connective tissue (30). Mechanotransduction through connective tissue with resultant effects on fibroblast cell shape and function was recently proposed as a mechanism for the therapeutic effect of acupuncture (29). Understanding the downstream cellular and molecular effects of mechanotransduction in loose connective tissue may therefore give key insights into the therapeutic mechanisms of a variety of treatments for musculoskeletal pain.

Our group recently showed (31) that, in mouse subcutaneous tissue excised and fixed immediately after death, fibroblasts have long branching processes and form an extensively interconnected cellular network. In the present study, we used ex vivo and in vivo mouse subcutaneous tissue models to investigate whether the morphology of this cellular network is responsive to changes in tissue length. We hypothesized that tissue stretch has an effect on fibroblasts' cell shape and that this effect is dependent on an intact cytoskeleton. We used quantitative morphometric analyses of histochemically stained

Address for reprint requests and other correspondence: H. M. Langevin, Dept. of Neurology, Univ. of Vermont College of Medicine, Given C423, 89 Beaumont Ave., Burlington, VT 05405 (E-mail: helene.langevin@uvm.edu).

The costs of publication of this article were defrayed in part by the payment of page charges. The article must therefore be hereby marked "*advertisement*" in accordance with 18 U.S.C. Section 1734 solely to indicate this fact.

tissue imaged with confocal microscopy, allowing differentiation of dendritic vs. expanded cell body morphologies. Unlike cell culture experiments, this in situ approach allowed examination of fibroblast cytoskeletal changes in a "native" environment where cell-matrix and cell-cell connections are maintained.

MATERIALS AND METHODS

Three complementary sets of experiments were performed: *1*) ex vivo experiments to evaluate the influence of tensile stretch on fibroblast morphology (as controls for these experiments, we evaluated tissue fixed before and after excision), *2*) in vivo experiments to evaluate whether stretch has similar effects on fibroblast morphology in vivo as ex vivo, and *3*) pharmacological experiments to evaluate which cytoskeletal elements contribute to altered fibroblast morphology under stretch. Our primary outcome measures were cell body cross-sectional area, cell body perimeter, cell field perimeter, cell body-to-field ratio, and cell body thickness (see *Confocal scanning laser microscopy and morphometric analysis* for detailed definitions). An additional secondary outcome measure was the number of cell-to-cell connections.

Ex vivo experiments. This series of experiments was performed to test the hypothesis that fibroblast cell morphology is affected by tensile stretch ex vivo. Twenty-three C57BL/6 mice (19–24 g) were killed by decapitation. Immediately after death, an 8 cm × 3 cm tissue flap containing dermis, subcutaneous muscle, and subcutaneous tissue was excised from the back of the mouse. The transverse length of the excised tissue sample was measured and marked on the skin of the mouse before excision. After dissection, the tissue flap's transverse length was measured again, with the tissue laying flat. The tissue flap was then placed transversely in grips (Fig. 1*A*) and immersed in HEPES-physiological saline solution, pH 7.4 at 37°C, containing (in mM) 141.8 NaCl, 4.7 KCl, 1.7 $MgSO_4$, 0.39 EDTA, 2.8 $CaCl_2$, 238.3 HEPES, 1.2 KH_2PO_4, and 5.0 glucose. The grips and tissue were then placed vertically in a holder (Fig. 1*B*) with the proximal grip connected to a 500-g (4.9 N)-capacity load cell. The distance between the two grips was measured with the tissue extended but loose and the load cell measuring zero. Unstretched tissue flaps were incubated at this length. Stretched tissue was elongated by advancing a micrometer connected to the distal tissue grip. The tissue was elongated at a rate of 1 mm/s until a load of 0.02 N was registered and then maintained at that length for the duration of the incubation. Incubation time for both stretched and unstretched tissue flaps was 10, 60, or 120 min. At the end of incubation, the tissue was immersion fixed in 95% ethanol for 1 h.

For control tissue fixed before excision, three C57BL/6 mice were killed by decapitation and immersed in 95% ethanol immediately after death. With the whole animal immersed, an incision was made along the dorsal and ventral midline from the neck to the tail and ethanol was slowly injected subcutaneously along the incisions, taking care not to force separation of the subcutaneous tissue layer during injection. The whole animal was kept immersed in fixative for 1 h. An 8 cm × 3 cm tissue flap was then excised from the back as above and immersion fixed for an additional 30 min. For control tissue fixed after excision, three C57BL/6 mice were killed by decapitation. Immediately after death, tissue flaps were excised from the back of the mouse as above and immersion fixed in 95% ethanol for 1 h.

In vivo experiments. These experiments were performed to verify that the effects of tissue stretch on fibroblast morphology observed ex vivo also occur in vivo. Six C57BL/6 mice were anesthetized with isoflurane. Once under anesthesia, each mouse was placed prone with its back curved laterally. The limbs on the left side of the body were restrained such that the distance from the left shoulder joint to the left hip joint was half the distance from the right shoulder joint to the right hip joint (Fig. 2). The right side was referred to as "extended" and the left side as "loose." The mouse was maintained in this position for 30 min while still under anesthesia and then killed by decapitation. Immediately after death, the whole animal was immersed in 95% ethanol, the skin was incised along the dorsal and ventral midline, and ethanol was injected subcutaneously through the incisions as described above. The whole animal was fixed for 1 h. Bilateral tissue flaps were then excised from the back and immersion fixed for an additional 30 min.

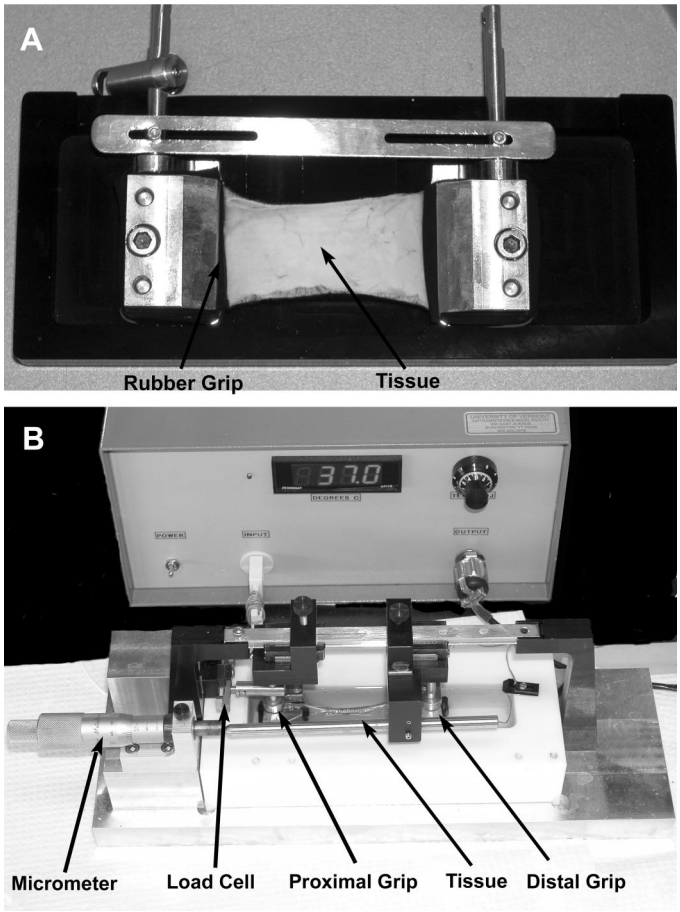

Fig. 1. Experimental setup. *A*: dissected mouse subcutaneous tissue with subcutaneous muscle and dermis still attached, laying flat on dermis side, held between 2 rubber grips, and secured with outer metal grips. *B*: dissected tissue in grips and mounted into the tissue stretching device. Bath heating control box is also shown.

Ex vivo pharmacological experiments. Tissue flaps were excised and placed into grips as in ex vivo experiments. Immediately after placement of the grips into the holder and with the tissue unstretched, either colchicine (Sigma, St. Louis, MO) or cytochalasin D (Sigma) was added to the incubation bath at a final concentration of 100 μM and 10 μM, respectively, followed by a 30-min incubation without stretch. After this, the tissue was further incubated, either stretched or unstretched, for an additional 2 h and then immersion fixed in 95% ethanol. Control samples were treated in the same manner but without the addition of inhibitors.

Histochemical staining. Phalloidin (a specific stain for polymerized actin) was used to visualize subcutaneous tissue fibroblasts with confocal microscopy for all ex vivo and in vivo experiments. After fixation, the tissue was rinsed overnight in phosphate-buffered saline (PBS), pH 7.4. Three subcutaneous tissue samples (each 10 mm × 10 mm) were dissected from the tissue flap. Each whole subcutaneous tissue sample was placed flat on a glass slide and stained with Texas red-conjugated phalloidin (4 U/ml; Molecular Probes, Eugene, OR) for 40 min at 4°C and then counterstained for 2 min with SYTOX

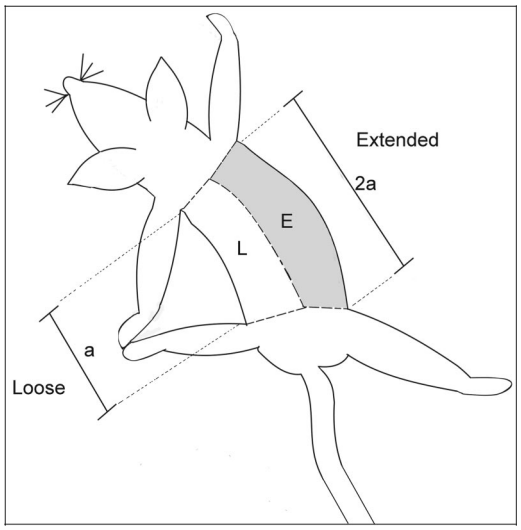

Fig. 2. In vivo tissue stretch experiment. Anesthetized mice were restrained for 30 min in a position such that the distance from the left shoulder joint to the left hip joint (*a*) was half the distance from the right shoulder joint to the right hip joint (2*a*). Tissue was excised on extended (E) and loose (L) sides.

Green (Molecular Probes) nucleic acid stain. Samples were mounted on slides with 50% glycerol in PBS with 1% *N*-propylgallate as a mounting medium and overlaid with a glass coverslip.

Confocal scanning laser microscopy and morphometric analysis. Histochemically stained subcutaneous tissue samples were imaged with a Bio-Rad MRC 1024 confocal microscope (Bio-Rad Microsciences, Hercules, CA) with a ×60 oil immersion lens (numerical aperture 1.4), 568-nm laser excitation, and iris aperture of 2.7. Each sample was divided into six roughly equal-sized areas, and one field was chosen at low power (×10) at the center of each area. For each field, a stack of 20 (313 μm × 313 μm) images was acquired at a 1-μm interimage interval. Image stacks were imported into the analysis software package MetaMorph (version 6.0; Universal Imaging, Downingtown, PA) for morphometric analysis. In each stack, all cells that were in focus in the 10th optical section (middle of stack) were measured. A cell was excluded if part of its cell body perimeter was outside the image. Cells were not identified as either fibroblasts or nonfibroblasts. Instead, all cells were measured, with the assumption that fibroblasts are the overwhelmingly predominant cell population in this tissue. An average of 26 (SD 9) cells were measured per excised tissue flap. For each cell, a wire frame of cell body perimeter and cell field perimeter was constructed (Fig. 3).

Cell body perimeter was defined as the outline of the cell's cytoplasm projected in the plane of the image excluding cell processes. A cell process was defined as an extension of a cell's cytoplasm longer than 2 μm and less than 2 μm in width at any portion of its length. Processes were identified in plane and out of

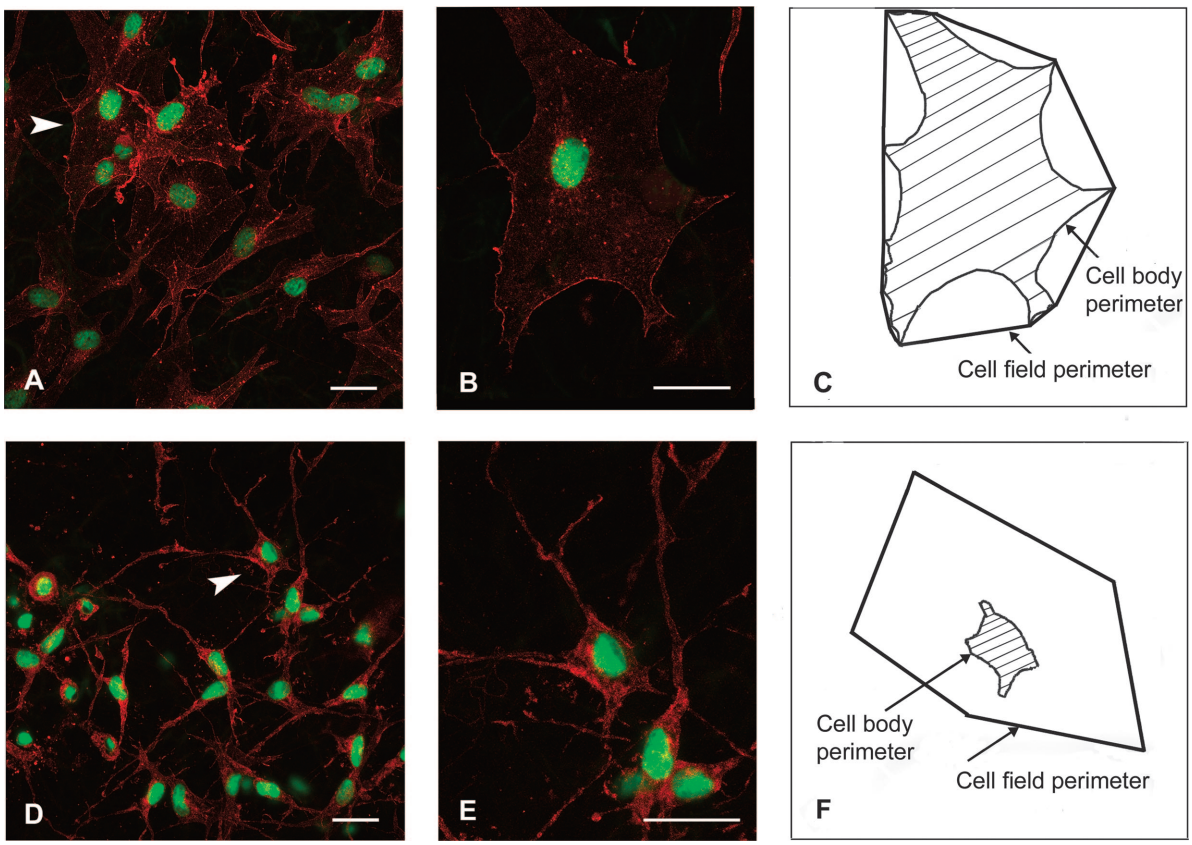

Fig. 3. Wire frames used in morphometric analysis. Mouse subcutaneous tissue incubated ex vivo with stretch (*A* and *B*) and without stretch (*D* and *E*) for 2 h, fixed with 95% ethanol, stained with phalloidin (red) and SYTOX (green), and imaged with confocal microscopy are shown. *A* and *D* are composite projections of stacks containing 20 optical sections taken at 1-μm intervals. *B* and *E* are projections of relevant optical sections containing the cells indicated by arrowheads in *A* and *D*, respectively. Scale bars, 40 μm. *C* and *F*: examples of wire frames for fibroblasts in stretched (*C*) and unstretched (*F*) tissue. The fibroblast in stretched tissue (*C*) has a "sheetlike" morphology with a high cell body cross-sectional area and high cell body-to-field ratio (ratio of cell body perimeter to cell field perimeter). In contrast, the fibroblast in unstretched tissue (*F*) has a "dendritic" morphology with a low cell body cross-sectional area and low cell body-to-field ratio.

plane by following each one through successive optical sections within the image stack. Cell body cross-sectional area was calculated as the area delimited by the cell body perimeter projected onto the image plane.

Cell field perimeter was defined as the sum of segments connecting the end of all visible cell processes. If a process extended from one cell to another, the midpoint of the process was chosen as the end of that process. The cell field perimeter was used in this study as an indication of the "territory" occupied by the cell, including cell processes. Note that in some cases where cell bodies were large and cell processes were short, the cell body perimeter could approach and even exceed the cell field perimeter (Fig. 2*B*).

Cell body-to-field ratio was calculated as the ratio of cell body perimeter to cell field perimeter. The cell body-to-field ratio was used in this study as an indication of the size of the cell body relative to the territory occupied by the whole cell including cell processes. A cell with a sheetlike morphology (large flat cell body and short processes; see Fig. 3, *A* and *B*) has both a high cell body area and a high cell body-to-field ratio. In contrast, a cell with a dendritic morphology (small cell body, long processes; see Fig. 3, *C* and *D*) is characterized by both a low cell body area and a low cell body-to-field ratio.

Cell body thickness was estimated by counting the number of individual optical sections in which the cell body cross-sectional area exceeded 4 μm^2, multiplied by the optical section thickness (1 μm).

For cell-to-cell connections, in a subset of images (tissue samples incubated ex vivo with and without stretch for 2 h) we also counted *1*) all "blind-ended" processes and *2*) all "joining" processes, defined as processes that appeared continuous with confocal microscopy (i.e., without a visible break from one cell to another) as previously described (31).

Statistical methods. For ex vivo experiments, two-way analyses of variance were used to test for differences between experimental conditions for each morphological outcome measure. The two factors represented stretch condition (stretch vs. no stretch) and incubation time (10, 60, and 120 min). If a significant interaction was detected, indicating that the effect of stretch was time dependent, comparisons between stretch and no-stretch conditions within each time point were performed with Fisher's least-significant difference (LSD) test. Dunnett's procedure, which controls type I error rate experimentwise, was used to compare each condition to tissue fixed before excision and after excision. Paired *t*-tests were used to compare extended and loose conditions for in vivo experiments. For all analyses, the experimental unit was considered the excised tissue flap, in which the observation represented the mean of all cell measurements made across multiple subcutaneous tissue samples and images. Statistical analyses were preformed with SAS statistical software (SAS Institute, Cary, NC). Significance was determined based on $\alpha = 0.05$.

RESULTS

Effect of pre- vs. postexcision tissue fixation. Mean transverse length of excised tissue samples was 6.2% (SD 2.1) shorter relative to in vivo transverse tissue length. In tissue fixed immediately after excision, fibroblast cell bodies were smaller in the plane of the tissue compared with cell bodies in tissue fixed by subcutaneous tissue injection before excision (Fig. 4, *A* and *B*). Mean cell body cross-sectional area, cell body perimeter, and cell field perimeter were 51%, 40%, and 37% lower, respectively, when tissue was fixed after excision

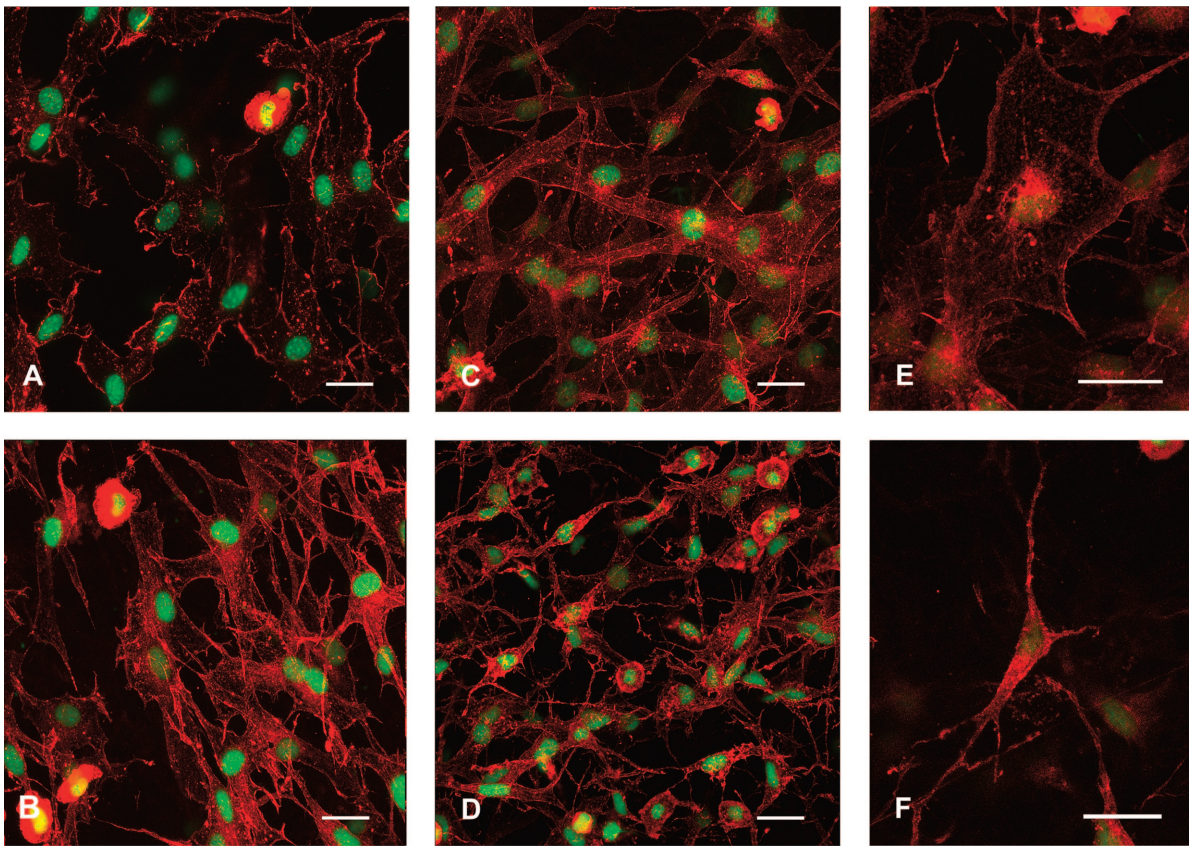

Fig. 4. *A* and *B*: mouse subcutaneous tissue fixed immediately before excision by subcutaneous injection of 95% ethanol (*A*) and after excision by immersion in 95% ethanol (*B*). *C* and *D*: mouse subcutaneous tissue incubated ex vivo for 2 h with stretch (*C*) and without stretch (*D*). *E* and *F*: individual fibroblasts in stretched (*E*) and unstretched (*F*) tissue. All samples shown were stained with phalloidin (red) and SYTOX (green). *A–D* are composite projections of stacks containing 20 optical sections taken at 1-μm intervals. *E* and *F* are projections of relevant optical sections containing the cells. Scale bars, 40 μm.

compared with before excision (Dunnett's procedure, $P < 0.05$ for outcomes) (Table 1, Fig. 5). However, the cell body-to-field ratio (ratio of cell body perimeter to cell field perimeter) was not significantly different between the two conditions. There was also no evidence of a difference in mean cell body thickness in tissue fixed before vs. after excision (Table 1).

Effect of tissue stretch ex vivo. Stretching the samples to a peak load of 0.02 N (equivalent to the weight of a 2-g mass) resulted in mean tissue elongation of 25.4% (SD 9.5) relative to the length of tissue extended but loose, with the load cell measuring zero. Fibroblasts in stretched tissue had large cell bodies similar to those fixed before excision (Fig. 4, *C* and *E*). In contrast, fibroblasts in unstretched tissue had markedly smaller cell bodies and longer processes (Fig. 4, *D* and *F*). Tissue stretch ex vivo had a significant time-dependent effect on fibroblast cell body perimeter and cell body cross-sectional area (ANOVA time by stretch interaction, $P < 0.01$). Both measures increased as a function of incubation time under stretch conditions and displayed no significant time effect under no-stretch conditions (Fig. 5). After a 2-h incubation time, mean cell body cross-sectional area and cell body perimeter were 201% and 75% greater, respectively, in stretched vs. unstretched tissue (Fisher's LSD, $P < 0.05$; Fig. 5, Table 1). Furthermore, the temporal increase observed for these measures under the stretch condition resulted in the 2-h time point not being significantly different from tissue fixed before excision (Dunnett's procedure; Table 1).

Tissue stretch ex vivo resulted in no significant effect on the cell field perimeter (ANOVA stretch effect, $P = 0.11$; Fig. 5). The size of the cell field perimeter significantly increased with duration of incubation independent of whether the tissue was stretched or unstretched (ANOVA time effect, $P = 0.009$). Mean cell field perimeters for both the stretched and unstretched 10-min incubation conditions were significantly different from those obtained from tissue before excision (Dunnett's procedure, $P < 0.05$; Table 1). Only the 120-min stretch condition resulted in a cell field perimeter significantly different from that obtained after excision (Dunnett's procedure, $P < 0.05$).

Tissue stretch also had a significant time-dependent effect on the cell body-to-field ratio (ANOVA time by stretch interaction, $P = 0.03$; Fig. 5). With increased incubation time, cell bodies in unstretched tissue became smaller relative to their cell field perimeter, whereas no significant time effect was observed in stretched tissue. Mean indexes for stretched and unstretched conditions were significantly different for the 2-h incubation time (Fisher's LSD, $P < 0.05$). When mean indexes of stretched and unstretched tissues were compared with preexcision and postexcision controls, the mean cell body-to-field ratio for the no-stretch 2-h condition was significantly different from that in both controls (Table 1).

Together, these morphological measurements show that fibroblasts in stretched tissue had a sheetlike morphology (increase in both cell body cross-sectional area and cell body-to-field ratio). In contrast, fibroblasts in unstretched tissue had a dendritic morphology with longer processes (decreased cell body cross-sectional area and cell body-to-field ratio). These changes in cell shape were reversible: fibroblasts in tissue stretched for 2 h and then incubated loose for an additional 2 h had a dendritic morphology similar to those in unstretched tissue (data not shown).

Tissue stretch resulted in a modest but significant decrease in fibroblast cell body thickness (across the plane of the tissue) that was independent of time of incubation (ANOVA stretch effect, $P = 0.04$). Overall mean cell body thickness was 8.05 and 6.55 μm for no-stretch and stretch conditions, respectively. There was no evidence that any of the experimental conditions differed from those obtained directly before or after excision (Dunnett's procedure). These results therefore show that 25% tissue elongation ex vivo caused fibroblast cell bodies to become slightly flatter (23% decrease) relative to the plane of the tissue.

There was no significant difference between stretch and no-stretch conditions in the mean number of cell processes (39 ± 4 and 41 ± 8 for stretch and no stretch, respectively) or the percentage of cell processes that were joining other cell processes ($27 \pm 3\%$ vs. $33 \pm 5\%$). This was only examined in tissue incubated for 2 h.

Effect of tissue stretch in vivo. Results of in vivo experiments examining the effects of tissue stretch on cell morphology paralleled the findings of the experiments conducted ex vivo. Tissue extended in vivo for 30 min had a significantly larger average cell body perimeter (paired *t*-test, $P = 0.01$) and a greater average cell body cross-sectional area (paired *t*-test, $P = 0.003$) compared with tissue that was loose in vivo for 30 min (Figs. 6 and 7, Table 2). Differences between extended and loose tissue conditions with respect to the average size of the cell field perimeter approached statistical significance (paired *t*-test, $P = 0.06$). As with ex vivo experiments incubated for

Table 1. *Morphometric measurements for ex vivo experiments*

			Ex Vivo Incubation					
			10 min		60 min		120 min	
	Fixed Preexcision	Fixed Postexcision	Stretch	No stretch	Stretch	No stretch	Stretch	No stretch
Sample size (*n*)	4	3	3	3	3	3	6	5
Cell body cross-sectional area, μm²	1,154.8±148.7†	557.8±80.6*	501.5±84.3*	449.6±64.5*	555.8±51.3*	415.0±30.7*	884.9±68.2†‡	294.1±56.1*
Cell body perimeter, μm	223.6±33.7†	133.8±8.0*	135.9±11.3*	135.9±11.5*	152.2±9.4*	127.0±0.4*	206.1±11.5†‡	118.0±11.3*
Cell field perimeter, μm	210.6±24.1†	132.1±7.7*	141.7±12.3*	147.3±3.1*	173.6±17.5	153.6±5.2	207.4±12.1†	168.2±12.2
Cell body-to-field ratio	1.00±0.06	1.03±0.01	0.99±0.01	0.95±0.07	0.92±0.07	0.82±0.07*	1.03±0.03‡	0.70±0.07*†
Cell body thickness, μm	7.1±0.5	6.2±0.7	7.2±0.6	7.4±0.7	6.6±1.6	9.1±0.6	5.9±0.7	7.7±0.5

Results presented as means ± SE. *Significantly different from fixed preexcision (Dunnett's procedure, $P < 0.05$); †significantly different from fixed postexcision (Dunnett's procedure, $P < 0.05$); ‡stretch significantly different from no stretch within time point (Fisher's least-significant difference test, $P < 0.05$).

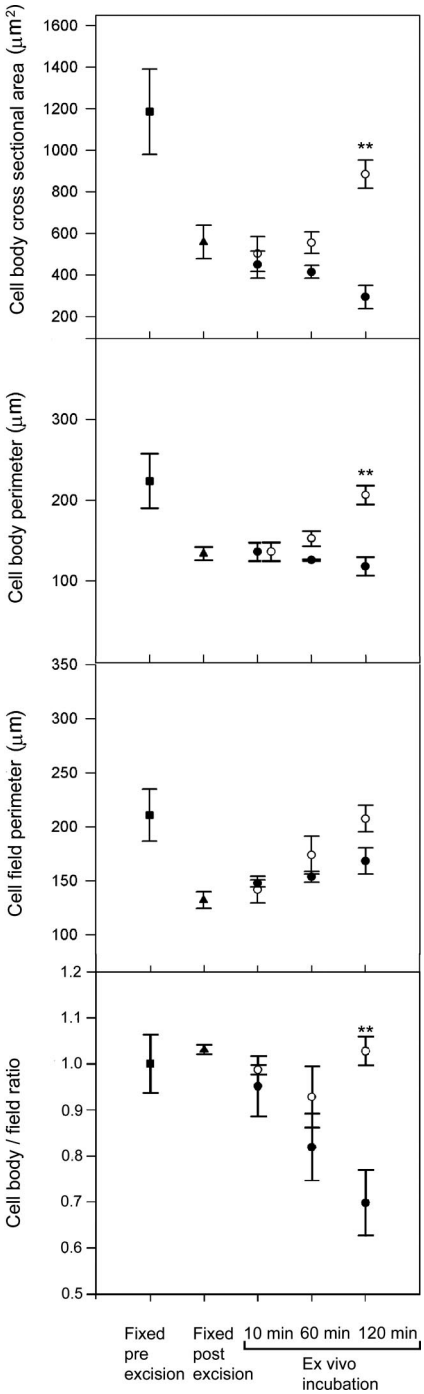

Fig. 5. Mean morphometric measurements for stretched (○) and unstretched (●) tissue during 10-, 60-, and 120-min ex vivo incubations. ■, measurements in tissue fixed before excision by subcutaneous injection; ▲, measurements in tissue fixed immediately after excision. **Significantly different from unstretched ($P < 0.01$). Error bars represent SE.

2 h, the cell body-to-field ratio was significantly lower in loose vs. extended tissue in vivo for 30 min (paired *t*-test, $P = 0.03$).

Ex vivo pharmacological experiments. Microtubules and actin microfilaments are principally responsible for rapid, dynamic changes in cell shape (17, 39). To test the contribution of these major cytoskeletal elements to the morphological response to tissue stretch, explants were incubated with and without stretch for 2 h in the absence or presence of colchicine (to disrupt microtubules) or cytochalasin D (to disrupt microfilaments). The morphology of fibroblasts in tissue stretched in the presence of either inhibitor was dramatically altered compared with control stretched tissue (Fig. 8, *A–C*), resembling more closely the morphology of cells in control unstretched tissue (Fig. 8*D*). In contrast, when colchicine and cytochalasin D were added in the absence of stretch, cell bodies remained small as in the unstretched control (Fig. 8, *D–F*). Therefore, both colchicine and cytochalasin D prevented the expansion of fibroblasts during stretch.

DISCUSSION

Subcutaneous tissue fibroblasts changed markedly in shape under the different experimental conditions. In tissue fixed by subcutaneous injection before excision, fibroblasts had a

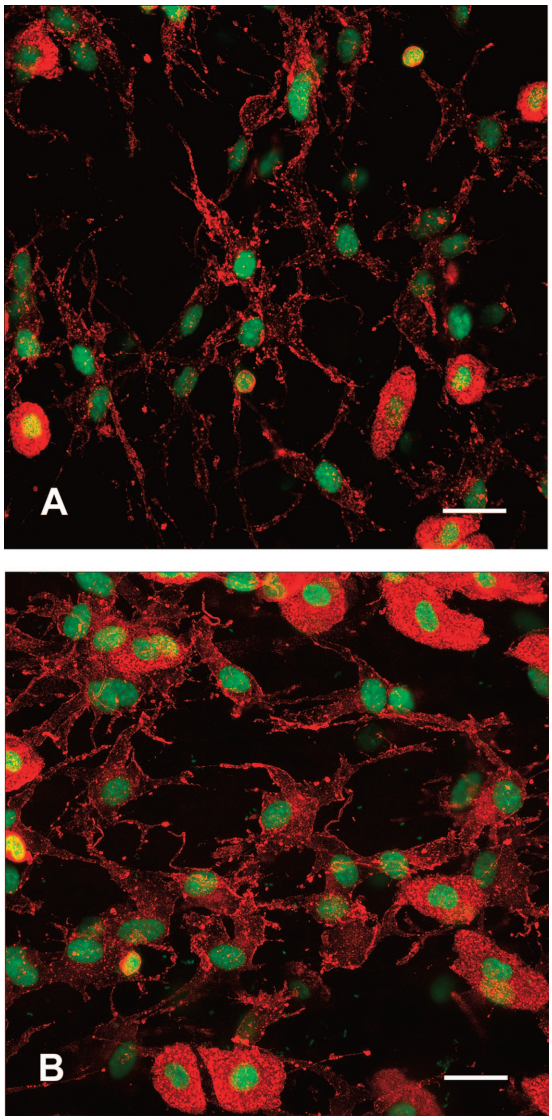

Fig. 6. Mouse subcutaneous tissue shortened (*A*) and elongated (*B*) for 30 min in vivo, followed by tissue fixation by subcutaneous tissue injection of 95% ethanol. Both samples were stained with phalloidin (red) and SYTOX (green). Images are composite projections of stacks containing 20 optical sections taken at 1-μm intervals. Scale bars, 40 μm.

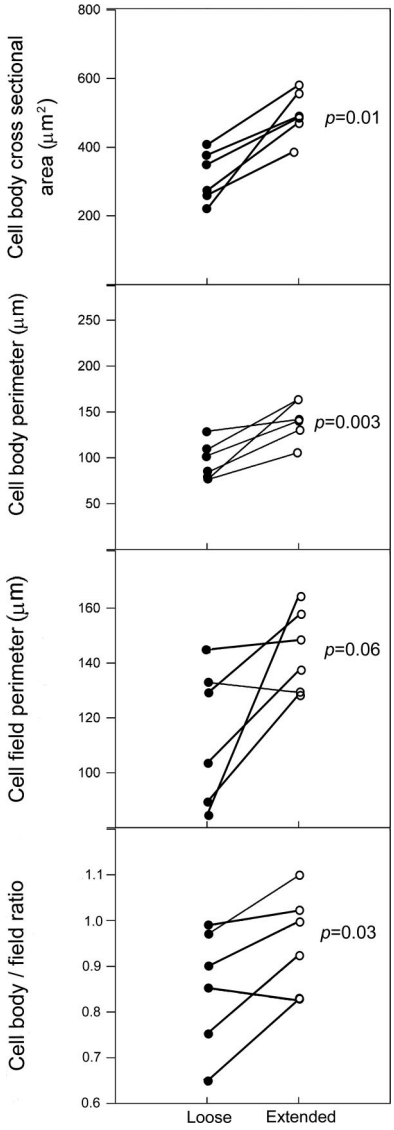

Fig. 7. Cell morphometric measurements of mouse tissue incubated shortened (loose, ●) vs. elongated (extended, ○) for 30 min in vivo. *P* values indicate significance associated with difference between loose and extended by paired *t*-tests.

sheetlike morphology with wide cell bodies and short processes, reminiscent of cultured fibroblasts grown on stiff, flat surfaces. When tissue length was shortened both ex vivo and in vivo, fibroblasts became more dendritic, with longer cytoplasmic processes and globular cell bodies, similar in morphology to fibroblasts grown in loose or 3D matrices. When tissue was stretched, fibroblast cell bodies became wider and flatter. Ex vivo results demonstrated that fibroblasts returned to their preexcision shape when the tissue was stretched, suggesting that fibroblasts within subcutaneous tissue normally are under some amount of tensile prestress (consistent with several biomechanical studies reporting the presence of prestress in skin; Ref. 36). However, in vivo results also showed that, in the body and under physiological conditions, subcutaneous tissue fibroblasts changed shape depending on whether the tissue was loose or extended. In addition to pronounced changes in cell shape, our results suggest that fibroblast cell bodies also changed in size during tissue stretch. Although we did not directly measure cell body volume in this study, the increase in cell body cross-sectional area with stretch was an order of magnitude greater than tissue lengthening (201% vs. 25%), whereas cell body thickness decreased by 23%. Even if fibroblast cell bodies behaved as completely compressible materials (Poisson's ratio = 0), such a large increase in cell body cross-sectional area could not have resulted passively from this amount of tissue deformation. Our results therefore show that connective tissue fibroblasts respond to changes in tissue length by active, pronounced, and reversible changes in both cell body size and overall cell shape.

In further support of an "active" mechanism underlying these changes in morphology, the addition of either colchicine or cytochalasin D to relaxed tissue prevented cell body expansion in response to subsequent tissue stretch. This suggests that both microtubules and microfilaments are necessary for stretch-induced cell body expansion. Although it is widely accepted that actin polymerization into microfilaments is the driving force for membrane and cell protrusion (5), work in recent years has shown an important synergy between microfilaments and microtubules in regulating dynamic changes in cell shape, for example, during cell motility and neuronal pathfinding (17, 18, 39). A particularly intriguing example is the demonstration that microtubules migrate into microfilament-coupled adhesion sites under high tensile stress (27). Thus both the cell geometry and inhibitor data presented above support a hypothesis in which tissue elongation exerts an initial stretch response in fibroblasts that stimulates a microfilament- and microtubule-dependent expansion of the cell body perimeter and acquisition of a larger, planar morphology.

Interplay between microtubules and microfilaments may also contribute to the apparent "contraction" of fibroblast cell bodies when tissue length was decreased. Although relatively little is known about the mechanisms governing the effects of matrix relaxation on cytoskeletal dynamics, it has been established that release of collagen gel tension can induce cultured fibroblasts to take on a spiny or dendritic morphology, with alterations in both microfilament and microtubule structure (20, 28). Furthermore, disruption of microtubules can elicit an increase in actomyosin-based contractility (15, 32), which may contribute to fibroblast contraction. Further experiments are needed to elucidate the biochemical mechanisms (including the respective roles of microtubules and microfilaments) that control cellular expansion and contraction responses to tissue tension.

Cytoskeleton-dependent changes in fibroblast shape in response to tissue stretch may have important implications for

Table 2. *Morphometric measurements for in vivo experiments*

	Loose	Extended
Sample size (*n*)	6	6
Cell body cross-sectional area, μm²	313.9±30.5	496.7±27.7*
Cell body perimeter, μm	95.8±8.6	136.3±7.7*
Cell field perimeter, μm	113.9±10.2	144.1±6.1
Cell body-to-field ratio	0.89±0.04	0.97±0.04*
Cell body thickness, μm	6.89±0.60	6.45±0.55

Results are presented as means ± SE. *Significantly different from loose (paired *t*-test, $P < 0.05$).

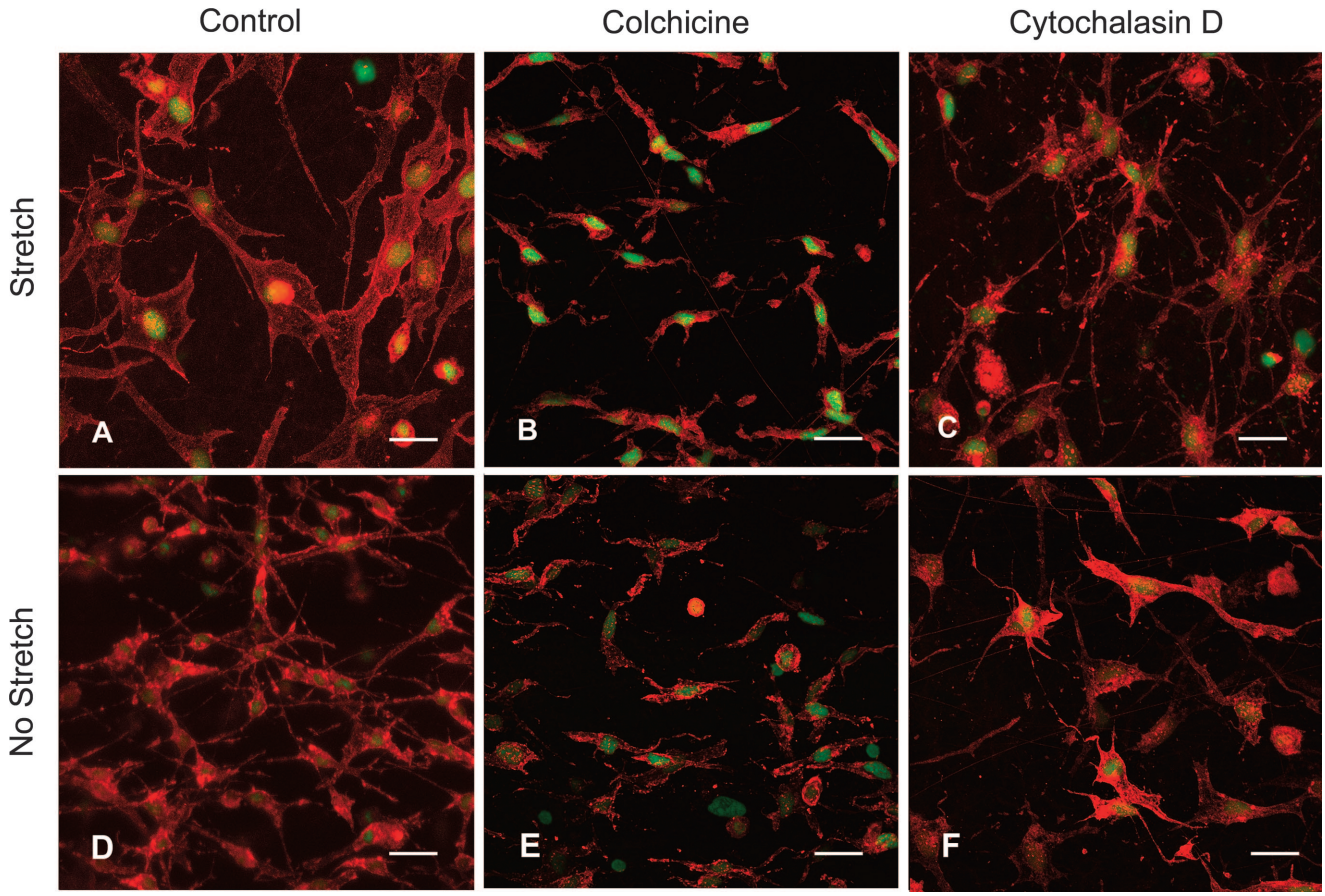

Fig. 8. Mouse subcutaneous tissue incubated for 2 h with stretch (*A–C*) and without stretch (*D–F*). Stretched and unstretched tissue samples were incubated without drugs (control; *A* and *D*), with 100 μM colchicine (*B* and *E*), or with 10 μM cytochalasin D (*C* and *F*). All samples shown were stained with phalloidin (red) and SYTOX (green). All images are composite projections of stacks containing 20 optical sections taken at 1-μm intervals. Scale bars, 40 μm.

intracellular signaling as well as cell-to-cell signaling within connective tissue. Intracellular signaling mechanisms are known to be intimately linked to the status of the cytoskeleton (1, 22). Disruption of actin cytoskeletal integrity can block signaling from cell surface receptors [e.g., receptor tyrosine kinases (2) and G protein-coupled receptors (14, 35)] and can also disrupt passage of signals from the cytoplasm into the nucleus (3). Synergy between signaling receptors, the cytoskeleton, and associated adhesion complexes is crucial for many aspects of normal cellular function (21, 22, 26). Hallmarks

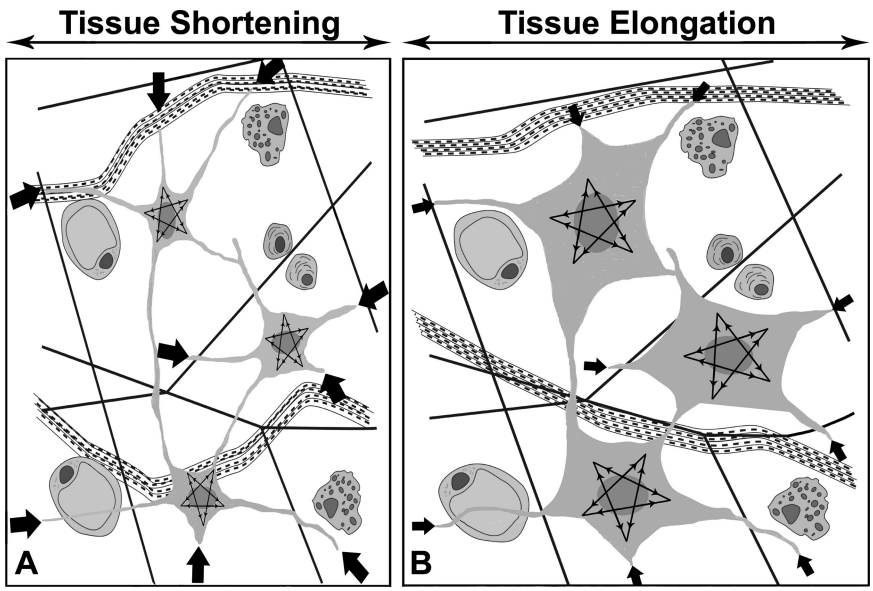

Fig. 9. Proposed model for fibroblast dynamic cytoskeletal response to tissue shortening and elongation with resultant cellular and tissue forces. Fibroblasts in elongated tissue (*B*) have a "sheetlike" morphology produced by microtubule assembly balanced by microfilament tension. Fibroblasts in shortened tissue (*A*) have a "dendritic" morphology resulting from microtubule disassembly in the presence of residual microfilament tension. Arrows inside fibroblasts represent internal cellular tension. Arrows outside fibroblasts represent the "pull" exerted by the cells onto the extracellular matrix.

include the establishment and maintenance of cell shape and position during embryonic development and modulation of cell shape in response to changes in the architecture of the extracellular environment (13, 16, 38). Indeed, elegant investigations have demonstrated that cytoskeleton-dependent changes in actual cell shape can also dramatically affect many cellular functions. These include signal transduction (9), mRNA and ribosome localization (11), transcriptional events (34), production of extracellular matrix (12), and cell adhesion dynamics (8). The consequences of regulating these individual functions manifest as shape-dependent control of higher-order cellular events such as cell division (9), survival (9), movement (5), differentiation (23), and the lineage commitment of stem cells (33).

Given our current results demonstrating the dramatic effect of tissue tension on fibroblast cell shape, along with the considerable evidence for the importance of shape and mechanotransduction in determining function at the cellular level (4), it is a natural extrapolation to consider the effect of aggregate cell shape on function at the tissue level (25). Loose connective tissue forms a bodywide tissue network. The fabric of this network, the collagenous extracellular matrix, is symbiotically linked to its resident cells, the fibroblasts, themselves interconnected in an extensive cellular network (31). In this study, we found no significant change in the average number of fibroblast processes making contact between cells under our different tissue length conditions. It is possible that stretching the tissue by >25% may disrupt fibroblast processes or cell-to-cell contacts. However, at the level of tissue stretch used in this study, our results suggest that, during fibroblast contraction, cytoplasmic retraction may have involved detachment of some cell-matrix connections but existing cell-to-cell connections were maintained. The significance of these connections, and how they are affected by mechanical forces, is at present unknown. The findings of Brown et al. (6, 7) also suggest the intriguing possibility that the connective tissue network may be contractile. These authors found that cultured fibroblasts respond to external loads by exerting contractile forces in the opposite direction to the applied load (6). Ingber (24) proposed a mechanism by which compressive forces borne by microtubules are transferred to extracellular matrix adhesions when microtubules are disrupted, thereby increasing substrate traction. Brown et al. (7) proposed that, by such a cytoskeletal "tensegrity" mechanism, fibroblasts balance "stored" internal cellular tension with matrix tension, thus maintaining tissue tensional homeostasis levels against opposing influences of external loading. The morphological and cytoskeletal changes found in this study are in agreement with this model, illustrated in Fig. 9. Another potentially important consequence of fibroblast responses to connective tissue tension may be homeostatic adjustment of interstitial fluid pressure and transcapillary fluid flow. Transmission of forces from fibroblasts to the extracellular matrix via focal adhesions has been shown to cause changes in interstitial hydrostatic pressure (40). Alterations in these functions may play an important role in the influence of mechanical forces on the response to injury and inflammation.

In summary, mouse subcutaneous tissue fibroblasts exhibited pronounced cytoskeleton-dependent changes in cell size and shape in response to tissue stretch both ex vivo and in vivo. These results show that both dendritic and sheetlike fibroblast phenotypes occur normally and interchangeably in vivo in response to changes in tissue length. On the basis of extensive evidence in cultured cells, these morphological changes are likely to be accompanied by important modification of cell signaling, gene expression, and matrix adhesion and may also produce variable connective tissue tension. Thus loose connective tissue may become more or less loose in response to changes in tissue length, and these dynamic changes may be accompanied by important changes in cellular and tissue biochemistry. The dynamic fibroblast responses to changes in tissue length demonstrated in this study have important implications for our understanding of connective tissue responses to changes in posture, normal movement, and exercise. These cellular events may also be key to the therapeutic mechanism of a wide variety of treatments using mechanical stimulation of connective tissue including physical therapy, massage, and acupuncture.

ACKNOWLEDGMENTS

The authors thank Kirsten N. Storch, Alexander T. Danco, and Debbie Stevens-Tuttle for technical assistance, as well as Douglas Gomez and Gilbert Gianetti of the University of Vermont Instrumentation and Model Making Facility. We also thank Drs. Marilyn J. Cipolla, Felix P. Eckenstein, and Kenneth R. Cutroneo for helpful suggestions.

GRANTS

The project reported in this article was supported by National Center for Complementary and Alternative Medicine (NCCAM) Research Grant R01-AT-01121. Its contents are solely the responsibility of the authors and do not necessarily represent the official views of the NCCAM, National Institutes of Health.

REFERENCES

1. **Aplin AE, Howe A, Alahari SK, and Juliano RL.** Signal transduction and signal modulation by cell adhesion receptors: the role of integrins, cadherins, immunoglobulin-cell adhesion molecules, and selectins. *Pharmacol Rev* 50: 197–263, 1998.
2. **Aplin AE and Juliano RL.** Integrin and cytoskeletal regulation of growth factor signaling to the MAP kinase pathway. *J Cell Sci* 112: 695–706, 1999.
3. **Aplin AE and Juliano RL.** Regulation of nucleocytoplasmic trafficking by cell adhesion receptors and the cytoskeleton. *J Cell Biol* 155: 187–191, 2001.
4. **Bershadsky AD, Balaban NQ, and Geiger B.** Adhesion-dependent cell mechanosensitivity. *Annu Rev Cell Dev Biol* 19: 677–695, 2003.
5. **Brock A, Chang E, Ho CC, LeDuc P, Jiang X, Whitesides GM, and Ingber DE.** Geometric determinants of directional cell motility revealed using microcontact printing. *Langmuir* 19: 1611–1617, 2003.
6. **Brown RA, Prajapati R, McGrouther DA, Yannas IV, and Eastwood M.** Tensional homeostasis in dermal fibroblasts: mechanical responses to mechanical loading in three-dimensional substrates. *J Cell Physiol* 175: 323–332, 1998.
7. **Brown RA, Talas G, Porter RA, McGrouther DA, and Eastwood M.** Balanced mechanical forces and microtubule contribution to fibroblast contraction. *J Cell Physiol* 169: 439–447, 1996.
8. **Chen CS, Alonso JL, Ostuni E, Whitesides GM, and Ingber DE.** Cell shape provides global control of focal adhesion assembly. *Biochem Biophys Res Commun* 307: 355–361, 2003.
9. **Chen CS, Mrksich M, Huang S, Whitesides GM, and Ingber DE.** Geometric control of cell life and death. *Science* 276: 1425–1428, 1997.
10. **Chicurel ME, Chen CS, and Ingber DE.** Cellular control lies in the balance of forces. *Curr Opin Cell Biol* 10: 232–239, 1998.
11. **Chicurel ME, Singer RH, Meyer CJ, and Ingber DE.** Integrin binding and mechanical tension induce movement of mRNA and ribosomes to focal adhesions. *Nature* 392: 730–733, 1998.
12. **Chiquet M, Renedo AS, Huber F, and Fluck M.** How do fibroblasts translate mechanical signals into changes in extracellular matrix production? *Matrix Biol* 22: 73–80, 2003.
13. **Danen EH and Sonnenberg A.** Integrins in regulation of tissue development and function. *J Pathol* 201: 632–641, 2003.

14. **Della Rocca GJ, Maudsley S, Daaka Y, Lefkowitz RJ, and Luttrell LM.** Pleiotropic coupling of G protein-coupled receptors to the mitogen-activated protein kinase cascade. Role of focal adhesions and receptor tyrosine kinases. *J Biol Chem* 274: 13978–13984, 1999.
15. **Elbaum M, Chausovsky A, Levy ET, Shtutman M, and Bershadsky AD.** Microtubule involvement in regulating cell contractility and adhesion-dependent signalling: a possible mechanism for polarization of cell motility. *Biochem Soc Symp* 65: 147–172, 1999.
16. **Giancotti FG and Tarone G.** Positional control of cell fate through joint integrin/receptor protein kinase signaling. *Annu Rev Cell Dev Biol* 19: 173–206, 2003.
17. **Goode BL, Drubin DG, and Barnes G.** Functional cooperation between the microtubule and actin cytoskeletons. *Curr Opin Cell Biol* 12: 63–71, 2000.
18. **Gordon-Weeks PR.** Microtubules and growth cone function. *J Neurobiol* 58: 70–83, 2004.
19. **Grinnell F.** Fibroblast biology in three-dimensional collagen matrices. *Trends Cell Biol* 13: 264–269, 2003.
20. **Grinnell F, Ho CH, Tamariz E, Lee DJ, and Skuta G.** Dendritic fibroblasts in three-dimensional collagen matrices. *Mol Biol Cell* 14: 384–395, 2003.
21. **Gumbiner BM.** Cell adhesion: the molecular basis of tissue architecture and morphogenesis. *Cell* 84: 345–357, 1996.
22. **Howe A, Aplin AE, Alahari SK, and Juliano RL.** Integrin signaling and cell growth control. *Curr Opin Cell Biol* 10: 220–231, 1998.
23. **Huang S and Ingber DE.** Shape-dependent control of cell growth, differentiation, and apoptosis: switching between attractors in cell regulatory networks. *Exp Cell Res* 261: 91–103, 2000.
24. **Ingber DE.** Tensegrity I. Cell structure and hierarchical systems biology. *J Cell Sci* 116: 1157–1173, 2003.
25. **Ingber DE.** Tensegrity II. How structural networks influence cellular information processing networks. *J Cell Sci* 116: 1397–1408, 2003.
26. **Juliano RL.** Signal transduction by cell adhesion receptors and the cytoskeleton: functions of integrins, cadherins, selectins, and immunoglobulin-superfamily members. *Annu Rev Pharmacol Toxicol* 42: 283–323, 2002.
27. **Kaverina I, Krylyshkina O, Beningo K, Anderson K, Wang YL, and Small JV.** Tensile stress stimulates microtubule outgrowth in living cells. *J Cell Sci* 115: 2283–2291, 2002.
28. **Kessler D, Dethlefsen S, Haase I, Plomann M, Hirche F, Krieg T, and Eckes B.** Fibroblasts in mechanically stressed collagen lattices assume a "synthetic" phenotype. *J Biol Chem* 276: 36575–36585, 2001.
29. **Langevin HM, Churchill DL, and Cipolla MJ.** Mechanical signaling through connective tissue: a mechanism for the therapeutic effect of acupuncture. *FASEB J* 15: 2275–2282, 2001.
30. **Langevin HM, Churchill DL, Wu J, Badger GJ, Yandow J, Fox JR, and Krag MH.** Evidence of connective tissue involvement in acupuncture. *FASEB J* 16: 872–874, 2002.
31. **Langevin HM, Cornbrooks CJ, and Taatjes DJ.** Fibroblasts form a body-wide cellular network. *Histochem Cell Biol* 122: 7–15, 2004.
32. **Liu BP, Chrzanowska-Wodnicka M, and Burridge K.** Microtubule depolymerization induces stress fibers, focal adhesions, and DNA synthesis via the GTP-binding protein Rho. *Cell Adhes Commun* 5: 249–255, 1998.
33. **McBeath R, Pirone DM, Nelson CM, Bhadriraju K, and Chen CS.** Cell shape, cytoskeletal tension, and RhoA regulate stem cell lineage commitment. *Dev Cell* 6: 483–495, 2004.
34. **Meyer CJ, Alenghat FJ, Rim P, Fong JH, Fabry B, and Ingber DE.** Mechanical control of cyclic AMP signalling and gene transcription through integrins. *Nat Cell Biol* 2: 666–668, 2000.
35. **Short SM, Boyer JL, and Juliano RL.** Integrins regulate the linkage between upstream and downstream events in G protein-coupled receptor signaling to mitogen-activated protein kinase. *J Biol Chem* 275: 12970–12977, 2000.
36. **Silver FH, Siperko LM, and Seehra GP.** Mechanobiology of force transduction in dermal tissue. *Skin Res Technol* 9: 3–23, 2003.
37. **Tamariz E and Grinnell F.** Modulation of fibroblast morphology and adhesion during collagen matrix remodeling. *Mol Biol Cell* 13: 3915–3929, 2002.
38. **Thiery JP.** Cell adhesion in development: a complex signaling network. *Curr Opin Genet Dev* 13: 365–371, 2003.
39. **Tirnauer JS.** Coupled zones of f-actin and microtubule movement in polarized cells. *Dev Cell* 3: 152–153, 2002.
40. **Wiig H, Rubin K, and Reed RK.** New and active role of the interstitium in control of interstitial fluid pressure: potential therapeutic consequences. *Acta Anaesthesiol Scand* 47: 111–121, 2003.